Characterization of a free-standing membrane supported superconducting Ti transition edge sensor

W. Zhang[1,2,*], W. Miao[1,2], Z. Wang[1,2], D. Liu[1,2], J.Q. Zhong[1,2], F. Wu[1,2], Q.J. Yao[1,2], X.H. Guo[1,2], S.C. Shi[1,2]
[1]*Purple Mountain Observatory, CAS, Nanjing, 210008, China*
[2]*Key Lab of Radio Astronomy, CAS, Nanjing,210008, China*
*Contact: wzhang@pmo.ac.cn, phone +86-25-83332229

Abstract—**Superconducting transition edge sensors (TES) based on a Ti microbridge on Si substrate have demonstrated a very low noise equivalent power (NEP). Their effective response time, however, is on the order of microsecond due to relatively high transition temperature (i.e. 300-400 mK) of the Ti microbridge, making it difficult to read out the signal of a large Ti TES array with a SQUID-based multiplexer. We propose a twin-slot antenna coupled superconducting Ti microbridge separated from the antenna feed and supported by a free-standing membrane. Its resistive transition (R-T) and current-voltage (I-V) curves are measured before and after wet etching of the Si substrate underneath the Ti microbridge. The free-standing membrane supported Ti TES shows slightly lower transitions and higher normal resistance. Its thermal conductance is reduced to ~150 pW/K from ~2000 pW/K. In addition, its effective response time measured with a current pulse signal is about 30 μs.**

INTRODUCTION

The THz and FIR band contains a wealth of information about the cold universe. Observations of gas and dust can probe the earliest stages in the formation of galaxies, stars, and planets. Due to the limited atmospheric transparency, a large-pixel detector array with high sensitivity is desirable for ground-based THz/FIR telescopes [1]. Purple Mountain Observatory is leading the efforts on a 5-m THz telescope (DATE5) [2] to be constructed at Dome A, the highest position on the Antarctic plateau at an elevation of 4100 m. Dome A has been confirmed to be an ideal site on earth for terahertz astronomy. We are currently developing a terahertz superconducting imaging array (TeSIA) for DATE5 at 350 μm [3], and TES is a potential detector candidate. Superconducting Ti TESs have demonstrated a very low optical NEP at 620 GHz [4], but its response time is on the order of microsecond due to relatively high transition temperature (i.e. 300~400 mK) of the Ti microbridge [5, 6], making it difficult to read out the signal of a large Ti TES array with a SQUID-based multiplexer. Thermal conductance between Ti microbridge and Si substrate should be further lowered to increase the effective response time. One way is to suspend the Ti microbridge from the substrate with legs for thermal isolation [7]. Here we propose a twin-slot antenna coupled superconducting Ti microbridge separated from the antenna feed and supported by a free-standing membrane. We present the details of the detector design, fabrication, electric characterization, and study the back etch effect on thermal conductance and response time.

DESIGN AND FABRICATION OF FREE-STANDING MEMBRANE SUPPORTED TI TES

Our design uses a twin-slot antenna to couple THz radiation (see Fig. 1b). The combination of twin-slot antenna and silicon elliptical lens has a nearly symmetric beam and linear polarization, which have been used successfully in THz heterodyne mixers [8, 9]. The electric field from each slot antenna propagates along coplanar waveguide (CPW) transmission line, then coherently added, and terminated at the Ti microbridge. The Ti microbridge works both as absorber and thermistor. The slot length, width and separation are 246 μm, 16 μm and 140 μm, respectively. Simulation shows that the twin-slot antenna is resonant at 345 GHz, and it is well matched with Ti TES with 30 Ω normal resistance via CPW transmission line.

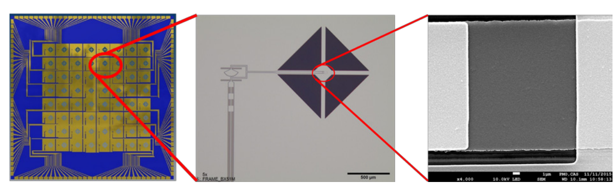

(a) (b) (c)

Fig. 1 (a) 8x8 superconducting Ti transition edge sensor array. (b) photo of the microbridge integrated with twin-slot antenna via CPW transmission line. (c) Ti microbridge with dimension of 16μm x16μm.

The superconducting TES devices are based on a Ti film, which is electron-beam evaporated on a 250-μm high-resistivity Si substrate in an ultrahigh vacuum environment. The microbridge is patterned by optical lithography. RF cleaning is used to remove the TiOx on the surface of Ti film before the deposition of 150 nm thick Nb contacts. The critical temperature of the Nb contacts is about 9K, so they serve as the Andreev reflection contact material. The Ti microrbidge is chosen to be 16 μm × 16μm, providing suitable saturation power (see Fig.1c). As shown in Fig.1a, we designed and fabricated a 8x8 superconducting Ti TES array. Fig. 1b shows a single-pixel Ti TES, including twin-slot antenna, RF choke filter, CPW transmission line, and Ti microbridge.

The fabricated Ti TES device is tested using an Oxford Triton 400 dilution cooler [10] that is able to cool the device down to 20 mK (see Fig. 2). The Ti TES wafer is anchored to the copper holder, then mounted on the mixing chamber (MC) stage. A temperature sensor is used to monitor the holder temperature. The constant voltage is realized with a 0.68-Ω shunt resistor (RSH) in parallel with the Ti TES device, which is then connected to the input coil of a Magnicon single-stage SQUID [11] on the 1K stage via twisted superconducting NbTi wires. The input inductance of the single-stage SQUID is 150 nH, and its current noise contribution is about 1 $pA/Hz^{0.5}$. The TES current is read out by the SQUID with a closed flux-locked loop.

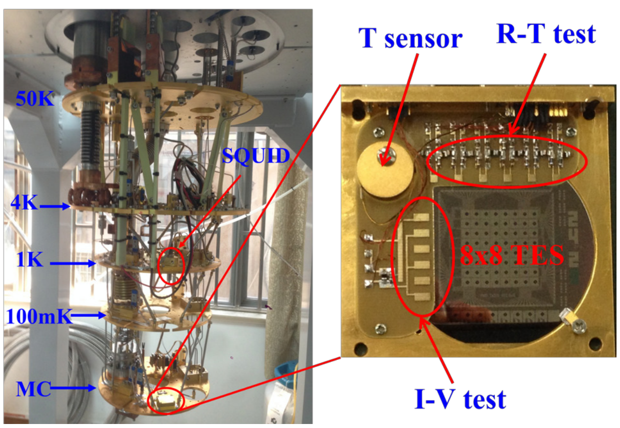

Fig. 2 Measurement setup for electrical properties of the Ti TES device. The TES device is mounted on the MC stage of dilution cooler. The TES current is read out using a single-stage SQUID operated at 1 K cold plate.

R-T CURVES

The resistance as a function of temperature is measured with an ac bridge. The results are shown in Fig.3. The resistance of Ti TES is about 1.6 KΩ at room temperature, and decreases with temperature. After Nb transition at ~9 K, the Ti microbridge shows a normal resistance of 2.3 Ω, consistent with sheet resistance of Ti film. There are two transition temperatures (i.e. 290 mK and 358 mK) from Ti microbridge and Ti/Nb contact pads, respectively. After KOH wet etch, the Ti TES device shows the same temperature dependence of its resistance, indicating that the Nb wire is not influenced by the KOH process. However, the normal resistance of Ti microbridge at 0.4 K is increased to 6.4 Ω, and the transition temperatures of Ti microbridge and Ti/Nb contacts are 266 mK and 338 mK, respectively. The superconductivity of Ti film is deteriorated by the KOH wet etch process. The reason is not clear and needs further study.

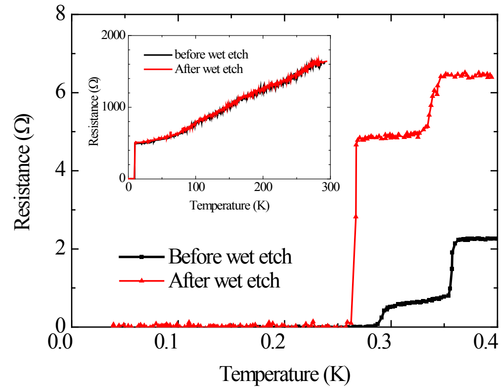

Fig.3 Measured resistance as a function of temperature of the Ti TES before and after wet etch

CURRENT-VOLTAGE CURVES

We measured the current–voltage characteristics of the Ti TES device at different bath temperatures between 50 mK and 350 mK (see Fig. 4). The current of the TES device (I_{TES}) can be directly obtained from the output voltage with the SQUID amplifier gain. Parasitic resistance (R_{PAR}) and normal resistance (R_N) are determined from its superconducting and normal branches of the I–V curves, respectively. The TES voltage (V_{TES}) is calculated through the Thevenin equivalent circuit model [12]. As plotted in Fig.4, there are several steps in the I–V curves in the transition regime, which might be due to the proximity effect. Superconductivity of the Ti film under the Nb contacts is indeed enhanced, leading to other transitions with higher critical temperatures in the measured resistive curve, which can be seen from the R-T curves in Fig.3. We choose the data points of the I–V curves at 1 Ω and plot the power level as a function of bath temperature (see Fig. 5).

The power flow from electrons to phonons follows $P_{DC} = K(T_c^n - T_{bath}^n)$, where P_{DC} is the DC bias power applied to the TES device, K a constant that depends on the geometry and material properties of the supporting structure, and n a thermal-conductance exponent depending on the dominant

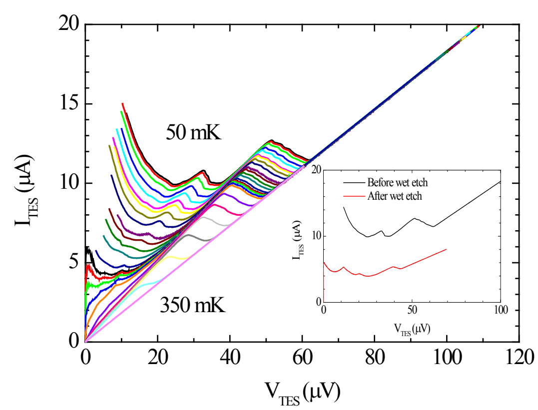

Fig. 4 I-V curves of the Ti TES at different bath temperatures before wet etch. The inset shows the I-V curves measured before and after KOH wet etch.

thermal transport mechanism. We can fit the measured DC power as a function of bath temperature to find K, n, and T_c. The best fit is obtained using $K=1.628\times10^4$ pW/K^n, n = 3.6 and T_c = 283 mK. Thermal conductance (G) between the TES device and the substrate can be calculated straightforwardly by $G = nKT_c^{n-1}$ =2219 pW/K. As n is close to 4, we indicate that the electron–phonon coupling is the dominant energy relaxation mechanism. After that, the Si substrate underneath the Ti microbridge was wet etched with KOH and the I-V curves were measured once again (see the inset of Fig. 4). The calculated thermal conductance (G) is reduced to 153 pW/K as shown in Fig. 5.

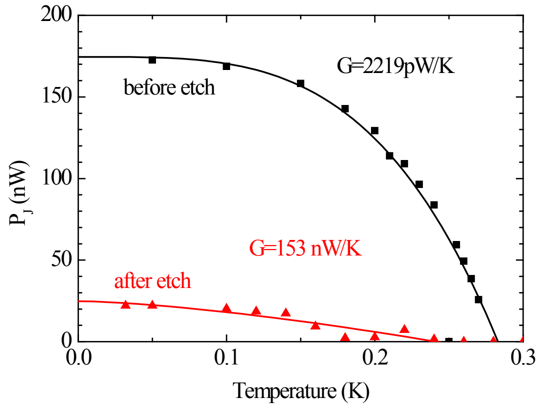

Fig.5 The power level as a function of bath temperature

As shown in the inset of Fig. 5, the two I-V curves show the similar shape. Due to the wet etch, the critical current is apparently reduced to about 5μA. This may be caused by the strain change of the TES device. After wet etch, n is reduced to 1.48 from 3.6, indicating that dominant thermal transport mechanism is diffusive phonon transport instead of electron-phonon interaction.

TABLE I
KEY PARAMETERS

	R_N (Ω)	T_c (K)	n	K	G (pW/K)	τ (μs)
Before etch	5.5	0.28	3.6	16280	2200	3
After etch	8.6	0.24	1.48	204	150	29

EFFECTIVE RESPONSE TIME

We then applied a current pulse with an amplitude much less than the bias current to the TES device at 2.66 μV, and measured its response. The rise and fall time of the current pulse is below 100 ns, which is much shorter than the measured response time. The decay curve can be fitted with an equation $V(t) = A_0+A_1\exp(-(t-t_0)/\tau_{eff})$, where A_0 and A_1 are the shift and the pulse height, t_0 and τ_{eff} are the current pulse incident time and response time, respectively. The best fitting value of the effective response time is τ_{eff} = 29 μs as shown in Fig.6. For comparison, the measured decay curve for a Ti TES without back etch is also plotted in the same figure. The effective response time is 3 μs, about 10 times faster than that with back etch.

Table 1 summarizes the main results of the Ti TES. After back etch, the thermal conductance is reduced from 2200 pW/K to 150 pW/K. Consequently, the effective response time is increased to about 30μs, 10 times larger than before. However, the KOH back etch has some influence on the superconductivity of Ti TES, the normal resistance becomes larger and the critical temperature shifts towards lower temperature, which should be studied further.

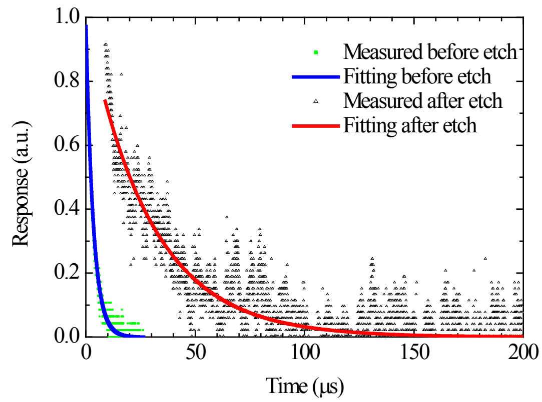

Fig.6 The measured and fitting pulse response of TES device before etch and after etch

CONCLUSION

We have studied the electrical performance of free-standing membrane supported superconducting Ti TES device. The thermal conductance extracted from the measured I–V characteristics at different bath temperatures is 150 pW/K as expected. As a result, the effective response time is 29 μs, ~10 times larger than that without back etch. We will further lower the thermal conductance by etching the SiN membrane into four legs, and the response time can be increased to 1ms, making it possible to use a SQUID-based time domain multiplexing to read out the signal of a 8x8 TES array.

ACKNOWLEDGMENT

The authors would like to thank W.Y. Duan and K. Zhang for their technical support. This work was supported in part by the NSFC under Grants 11127903, 11190012, 11473075, by the Chinese Academy of Sciences under Grant XDB04010300, and by the operation, maintenance and upgrading fund for astronomical telescopes and facility instruments.

REFERENCES

[1] W. S. Holland et al., “SCUBA-2: The 10000 pixel bolometer camera on the James Clerk Maxwell Telescope,” Mon. Not. R. Astron. Soc., vol. 430, p. 2513, 2013

[2] J. Yang, Y.X. Zuo, Z. Lou, J.Q. Cheng, Q.Z. Zhang et al., Res. Astron. Astrophys. 13(12), 1493–1508 (2013).

[3] S.C. Shi, W. Zhang, J. Li, W. Miao, Z.H. Lin, Z. Lou, and Q.J. Yao, "A THz superconducting imaging array developed for the DATE5 telescope", J. Low Temp. Phys.vol. 184, 2016.

[4] B.S. Karasik, R. Cantor, "Demonstration of high optical sensitivity in far-infrared hot electron bolometer," Appl. Phys. Lett. **98**, 193503, 2011.

[5] B. S. Karasik, S.V. Pereverzev,D. Olaya, M. E. Gershenson, R. Cantor, J. H. Kawamura, P. K. Day, B. Bumble, H. G. LeDuc, S. P.Monacos, D. G.

Harding, D. Santavicca, F. Carter, and D. E. Prober, “Development of the nano-HEB array for low-background far-IR applications,” in Proc. SPIE, vol. 7741, p. 774119, 2010.

[6] W. Zhang, J.Q. Zhong, W. Miao, Z. Wang, D. Liu, Q.J. Yao, S.C. Shi, T.J. Chen, M.J. Wang, "Electrical chracteristics of superconducting Ti transition edge sensors," J. Low Temp. Phys, 184,11-16, 2016.

[7] M.J. Myers, W. Holzapfel, A.T. Lee, R. O'Brient, P.L. Richards, and H.T. Tran, "An antenna-coupled bolometer with an integrated microstrip bandpass filter," Appl. Phys. Lett. 86, 114103, 2005.

[8] W. Zhang, J.R. Gao, M. Hajenius, W. Miao, P. Khosropanah, T.M. Klapwijk, and S.C. Shi, "Twin-slot antenna coupled NbN hot electron bolometer mixer at 2.5 THz" IEEE Trans. Terahz. Sci. Tech. vol.1 (2), pp.378-382, 2011.

[9] W. Zhang, D. Hayton, J.R. Gao, M. hajenius, W. Miao, D. Liu, T.M. Klapwijk, and S.C. Shi, "Optimized sensitivity and beam pattern of a twin-slot antenna coupled NbN HEB mixer at 1.6THz," in Proc. SPIE, vol. 8452, p. 84522H, 2012.

[10] Triton TM 200/400, Cryofree dilution refrigerator, Issue 3.0 (Oxford Instruments, 2012)

[11] *High performance DC SQUID electronics, XXF-1 manual*, v3.3.11. Magnicon Phys. Res. Instrum., Hamburg, Germany (2013)

[12] K. D. Irwin and G. C. Hilton, “Transition-edge sensors, in Cryogenic Particle Detection,” in *Topics in Applied Physics*, vol. 99. Berlin, Germany: Springer-Verlag, 2005.